Electrochemical behavior, structural, morphological, Calf Thymus-DNA interaction and *in-vitro* antimicrobial studies of synthesized Schiff base transition metal complexes

A. Palanimurugan [a], A. Dhanalakshmi [b], P. Selvapandian [a], A. Kulandaisamy [a],*

[a] *Department of Chemistry, Raja Doraisingam Government Arts College, Sivagangai, 630 561, Tamilnadu, India*
[b] *Department of Physics, Raja Doraisingam Government Arts College, Sivagangai, 630 561, Tamilnadu, India*

ABSTRACT

New tetradentate Schiff base transition metal complexes have been derived from salicylidene-4-imino-2,3-dimethyl-1-phenyl-3-pyrazolin-5-one and histidine were characterized by CHN analysis, magnetic susceptibility measurements, molar conductance, FAB-MS, IR, ^{1}H-NMR, UV, CV, EPR, Fluorescence emission, AFM and Powder XRD techniques. AFM images and Powder XRD data endure that the complexes are nano-size grains with poly-crystalline structure. The spectral evidences showed that all the metal chelates are square planar geometry except [VOL] complex which exist square-pyramidal geometry. Electrochemical data (CV) for [CuL] and [VOL] complexes in acetonitrile solution indicates that the redox potential of metal ions is affected by the coordinated ligand. Electron Spin Resonance (ESR) spectra of [CuL] and [VOL] complexes were well coinciding with proposed geometries and other reported complexes. CT-DNA interaction studies of [CuL] complex reveals that an intercalation binding mode occurs between complex and DNA base pairs. The *in vitro* antimicrobial activity of complexes has been tested against the growth of some fungal and bacterial species persist that chelates have better control than ligand.

1. Introduction

Schiff base and its metal complexes derived from 4-aminoantipyrine are essential because of their important applications in biochemical, biological, catalytical, analytical and industrial field. Besides, tetradentate Schiff base metal complexes composed of (N_2O_2) donor atoms are crucial chelating ligands for scheming catalytically and medicinally useful metal chelates [1, 2, 3, 4, 5, 6]. Amino acids and its derivatives can have some extent ligand due to their good solubility properties and biological transports. Among amino acids, histidine is very significant bioactive amino acid with plentiful physiological functions and the tendency to take on interaction with proteins [7, 8, 9, 10]. They can probably to form Schiff bases at beyond their isoelectric point with 4-aminoantipyrine derivatives. The ensuing product acts as polydentate ligands and readily forms complexes with metal ion. Schiff base complexes with imines have deserved much attention, probably because of their ability to intercalate between the bases of DNA and to participate in catalytic cycles with usual reducing and oxidizing agents in biological medium and Cu(II) is also involved in the causation and cure of cancer

[11, 12, 13, 14, 15, 16]. This prompted us to synthesize a new series of heterocyclic compounds containing the antipyrinyl moiety from the Schiff bases derived from the condensation of Salicylidene-4-iminoantipyrine and Histidine [17, 18, 19, 20, 21, 22, 23, 24, 25, 26]. In this paper, we report the synthesize, structural characterization, CT-DNA interaction and biological screening investigation of copper, nickel, cobalt, oxovanadium and zinc complexes with Schiff base prepared by Salicylidene-4-iminoantipyrine and Histidine.

2. Experimental

2.1. Material and methods

4-aminoantipyrine, Salicylaldehyde, Histidine and all metal chloride salts were procured from Merck (Darmstadt, Germany). Solvents used for electrochemical and spectroscopic studies have been purified by standard [27] procedures. Himedia chemicals were used as such for antimicrobial studies. CT- DNA was purchased from Genei Bangalore (India). Ethidium bromide (EB) and Agarose (molecular biology grade) were obtained from

---

Sigma–Aldrich (St. Louis, Missouri, USA). Tris (hydroxymethyl)amino-methane hydrochloride (Tris–HCl) buffer solution was prepared using deionized and distilled water.

2.2. Instrumentation techniques

Elementar Vario EL III Carlo Erba 1108 analyzer is used to carried out elemental analysis (C, H and N) and Mass Spectrometers Jeol SX-102 (FAB) in a 3-nitrobenzylalcohol matrix for determination of molecular weight by Fast atomic bombardment mass spectra (FAB-MS). X-band ESR spectra of the [CuL] and [VO(IV)L] complexes in dimethyl sulphoxide solution at 77 K were recorded on a JEOL 47 series ESR spectrometer. ^{1}H-NMR spectra of the Schiff base and its [ZnL] complex were recorded on a Bruker Advance DRX 300 FTNMR spectrometer using deutrated chloroform solvent (TMS-standard). AFM was recorded in Bharathidasan University, Trichy. Cyclic voltammogram and Powder XRD patterns (XPERT-PRO) were recorded at Alagappa University, Karaikudi. CHI 620C electrochemical analyzer was used for electrochemical measurements. It has three electrode systems; Hg/Hg_2Cl_2 as reference electrode, glassy carbon electrode as working electrode and platinum wire as auxiliary electrode. Tetrabutyl ammonium perchlorate was used as supporting electrolyte. The solutions were deoxygenated by purging with N_2 prior to measurements. Molar conductance of the metal chelates (10^{-3} M) was measured at 25 °C using Model-601 Deepvision digital conductivity meter. Magnetic susceptibility measurements of metal chelates were carried out by employing Gouy balance at 25 °C $CuSO_4.5H_2O$ was used as calibrant. Thin layer chromatography is used to check the purity of Schiff base and its complexes [28].

2.3. Synthesis of Schiff base

An ethanolic solution (40 mL) of 3.14 g Salicylidene-4-iminoantipyrine (10 mmol) and 1.55 g Histidine (10 mmol) was refluxed on water bath for about 12 h in the presence of 1 mL piperidine. The resulting solution was concentrated by keeping the mixture under water bath. On cooling, the solid product formed was filtered and recrystallized in methanol.

2.4. Synthesis of Schiff base metal complexes

Schiff base (2.565g, 5 mmol) and Metal chloride salts (5 mmol) was dissolved in 50 mL of ethanol and the mixture was boiled under reflux for about 6 h. The solvents were reducing to one third by evaporation on a water bath. The resultant concentrated solution was stirred with 10 mL of petroleum ether (40–60 °C range). The precipitated complexes formed were separated by filtration, washed with ethanol and petroleum ether. Finally, the complexes were recrystallized in $CHCl_3$ and dried in vacuo.

2.5. Antimicrobial assay

In-vitro antimicrobial activities of the H_2L [CoL] [NiL] [CuL] [ZnL] and [VOL] complexes were tested against two Gram-positive (*Staphylococcus aureus* and *Bacillus subtilis*) and three Gram-negative (*Escherichia coli, Klebsiella pneumoniae* and *Salmonella typhi*) bacterial and antifungal activity against *Aspergillus flavus, Aspergillus niger, Candida albicans, Rhizoctonia bataicola* and *Rhizopus stolonifer* by disc diffusion method using nutrient agar for bacteria and potato dextrose agar for fungi as medium respectively. The stock solutions (10^{-2} mol L^{-1}) were prepared by dissolving the compounds in dimethyl formamide and the solutions were serially diluted in order to find the Minimum Inhibitory Concentration (MIC) values. In a usual procedure, a disc made on the agar medium which is previously inoculated with microorganisms [29]. The prepared compounds were tested against some fungi (72 h) and bacteria (48 h) to provide the minimum inhibitory concentration (MIC) for each compound. During this period, the test solutions were diffused and growth of inoculated microorganisms was affected. The inhibition zone

was developed at which the concentration was noted. Nystatin and Tetracycline were used as standard control drugs for fungi and bacteria respectively.

2.6. CT-DNA interaction studies

The solutions of CT-DNA in Tris-HCl and NaCl buffer (pH = 7.3) in water with a ratio 1.9 of $A260/A280$ UV absorbance, signifying that the DNA was suitably liberated from protein. For 25 cycles sonicated, concentrated stock DNA solutions prepared in buffer and 30 s each cycle consistence with minute intervals. The CT-DNA concentration was measured by its molar extinction coefficient at 260 nm after required dilutions. DNA stock solutions were stored at 4 °C and used within a day [CuL] complexes/CT-DNA was prepared by dissolving in alcohol and diluted with buffer solution to the requisite concentration for all the desired experiments. For absorption spectra and cyclic voltammogram experiments, the DNA solutions were pretreated with the solution of the complex to ensure no change in their concentration [30, 31, 32, 33, 34].

2.6.1. UV-Visible spectral studies

UV-Visible spectra were collected by adding specific amount of [CuL] complex solution in various concentration of CT-DNA solution. The absorbances were measured after the baseline correction by Tris-HCl buffer solution, then the successive addition of CT-DNA pretreated with the complex.

2.6.2. Cyclic voltammetric studies

In CV studies, the glassy carbon electrode was modified by adding a droplet of 2μL of 5×10^{-3} M of CT-DNA on the electrode surface and dried. Then the electrode was rinsed with distilled water. Pt wire as auxiliary electrode, Ag/AgCl as standard electrode and a CT-DNA modified glassy carbon electrode was used as a working electrode. A known concentration of freshly prepared complex solution was used to record and compared with CV of CT-DNA and [CuL] complex.

3. Results and discussion

Physical characterization, analytical, magnetic susceptibility data and magnetic moment values of Schiff base and its complexes were given in Table 1. The synthetic pathway for the compounds is shown in Schemes 1 and 2.

The analytical data of metal complexes correspond well with the general formula [ML], where L = $C_{24}H_{24}N_6O_3$; M = Co(II), Ni(II), Cu(II), Zn(II) and VO(IV). The paramagnetic nature of the metal complexes was confirmed from their magnetic susceptibility data. The lower conductance of the complexes supports their non-electrolytic natures [35].

3.1. Mass spectra

FAB-Mass spectra was evidently obtained for Schiff base ($C_{24}H_{24}N_6O_3$) and showed a molecular ion peak of at m/z 511, as expected for a monomeric formulation of the respective ring. Moreover [$CuC_{24}H_{22}N_6O_3$] complex which exhibited a molecular ion peak at m/z 573, which confirms the expected stoichiometric composition of the formation of complex as [ML]. Elemental analyses values (Table 1) are in completely close agreement with the calculated values from molecular formulae assigned to these complexes which are further supported by FAB-Mass spectra of other complexes.

3.2. Powder XRD

XRD patterns of Schiff base (H_2L) and its [CuL] [NiL] and [ZnL] complexes were shown in Fig. 1. From Fig. 1a, Schiff base shows different peaks started from 10.1641° to 51.8425° positions suggest that it has sharp polycrystalline structure. The 100 % intensity peaks for Schiff base (Fig. 1a) [CuL] (Fig. 1b) [NiL] (Fig. 1 c) and [ZnL] (Fig. 1d) complexes

Table 1
Physical characterization, analytical, molar conductance, magnetic susceptibility data and magnetic moment value of Schiff base (H_2L) and their complexes.

Compound	Colour	M. P °C	% Found (Calculated)				$\Lambda m\ 10^{-3}\ (\Omega^{-1}\ cm^2\ mol^{-1})$	μ_{eff} (BM)
			M	C	H	N		
H_2L	Pale Yellow	153	-	62.25 (62.29)	5.58 (5.61)	19.60 (19.63)	-	-
[CoL]	Pale Pink	230	10.54 (10.57)	51.57 (51.61)	4.28 (4.30)	15.02 (15.05)	1.6	3.84
[NiL]	Brown	246	10.52 (10.57)	51.60 (51.61)	4.24 (4.30)	15.03 (15.05)	1.42	-
[CuL]	Pale Brown	209	11.33 (11.39)	51.12 (51.15)	4.23 (4.26)	14.90 (14.92)	1.2	1.76
[ZnL]	Green	214	11.50 (11.52)	51.02 (51.06)	4.22 (4.26)	14.87 (14.89)	1.64	-
[VOL]	Pale Green	238	8.98 (9.01)	50.86 (50.88)	4.21 (4.24)	14.80 (14.84)	1.51	1.83
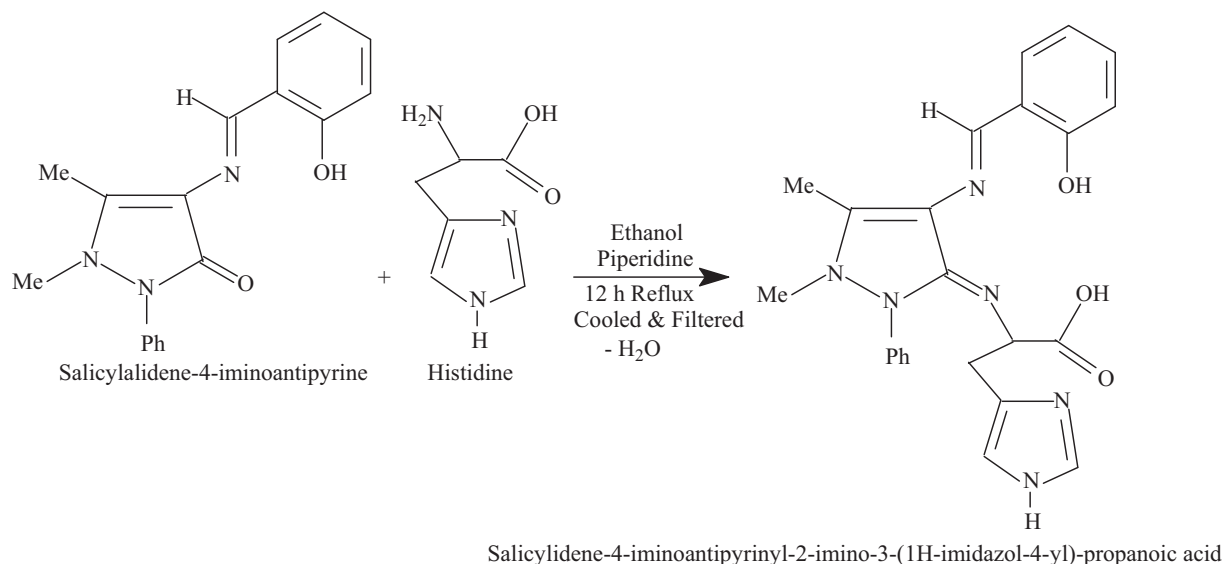
Scheme 1. Preparation of Salicylidene-4-iminoantipyrinyl-2-imino-(1H-imidazol-4-yl)-propanoic acid.

were appeared at 13.5218°, 31.7020°, 31.7626° and 29.8245° respectively. Some new peak positions appearance and higher intensity of all the complexes indicate that the metal ions were coordinated with ligand. The peak intensity of Schiff base at 13.5218° region is reduced in all chelates also supports the above actuality. Broaden peaks in all complexes confirms that the quantum confinement of Schiff base in chelates due to the attachment of donor atoms to metal ions.

The average crystallite size (d_{XRD}) of the complexes was calculated using Scherrer's formula [36]. The Schiff base (H_2L) [CuL] [NiL] and [ZnL] complexes have an average crystallite sizes of 64, 54, 55 and 42 nm respectively. The decrease in intensity of these peaks in [CuL] [NiL] and [ZnL] complexes represents the reduced crystalline size with increasing full width half maximum (FWHM) values [37, 38]. From the correlation of XRD spectra, the observed average crystalline size of Schiff base is somewhat higher than metal complexes and these reduced average crystalline sizes of metal complexes leads to better antibacterial activities than Schiff base [39].

3.3. Morphological study

Atomic Force Microscopy (AFM) images for Schiff base and its complexes represented in Fig. 2 (a) - (d). The scanning area (surface roughness) in both nano meter and micro meter scale was taken and recorded for Schiff base and metal complexes. At the left side of each image, an intensity scale is shown that indicating the height and depth along the z-axis. In Fig. 2a, all the AFM images showed well defined sized spherical particles [40]. Obviously, by the introducing metal in Schiff base [CuL] complex has modified surfaces to uniform sized smooth spherical shape as indicated in Fig. 2(b).

The [NiL] complex (Fig. 2(c)) indicated that the surface which was

more uniform in small spherical grains. Fig. 2(d) showed [ZnL] complex has too smooth and uniform surface with nano ball like structure. The Schiff base (H_2L), [CuL], [NiL] and [ZnL] complexes have an average crystallite sizes of 64, 54, 55 and 42 nm respectively which is confirmed by powder XRD. The surface quality of Schiff base could be enhanced by the incorporated metal complexes. This is possibly due to the fact that the metal complexes plays a vital role through the formation of Schiff base which makes it have more uniform and smooth surfaces.

3.4. IR spectra

IR spectrum of Schiff base shows a weak broad band at 3500- 3100 cm^{-1} region which is assigned to hydrogen bonded phenolic –OH group of salicylaldehyde and –COOH group of histidine moiety. The absence of bands revealed that the deprotonation when chelation. The cyclic –NH-group of histidine moiety present in ligand system and a weak node due to merging of –OH groups appeared a new strong band at 3090 cm^{-1} in all metal complexes. It confers the free groups and is not involved in ligand coordination with metal ion. –C=N groups of the Schiff base, the strong bands at 1615 - 1600 cm^{-1} regions. The appearance of band at 1591 - 1512 cm^{-1} region indicates azomethine nitrogen coordinated to the metal. These lower frequencies in all metal complexes have possible drift of lone pair electron density towards the metal ion [41]. Besides, the peak appeared at 1630 cm^{-1} region for –C=O of acid group in histidine moiety indicated the existence of –C=O group in Schiff base and all metal complexes. All the metal complexes show the new peaks at 510 cm^{-1} and 430 cm^{-1} region due to the formation of M-N and M-O bonds. The [VO(IV)L] complex shows at 960 cm^{-1} region [42] which corresponds well it characteristic V=O frequency in addition to other bands.
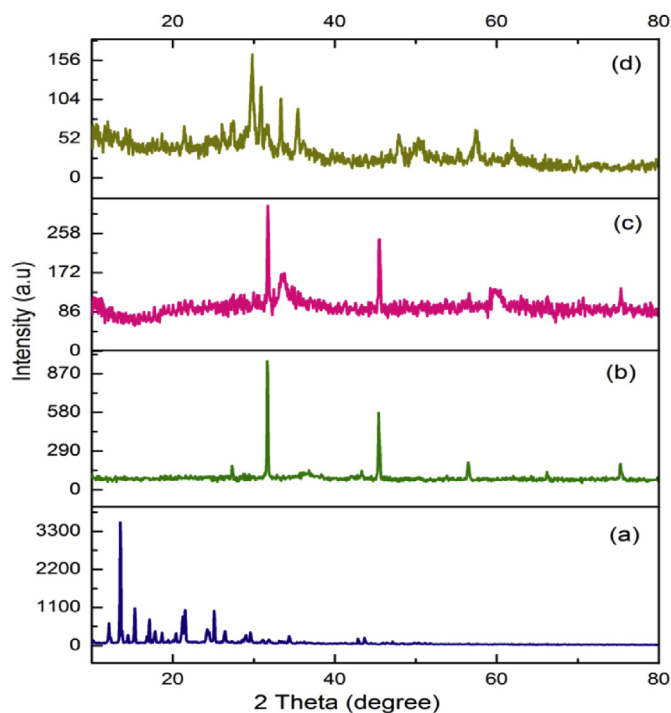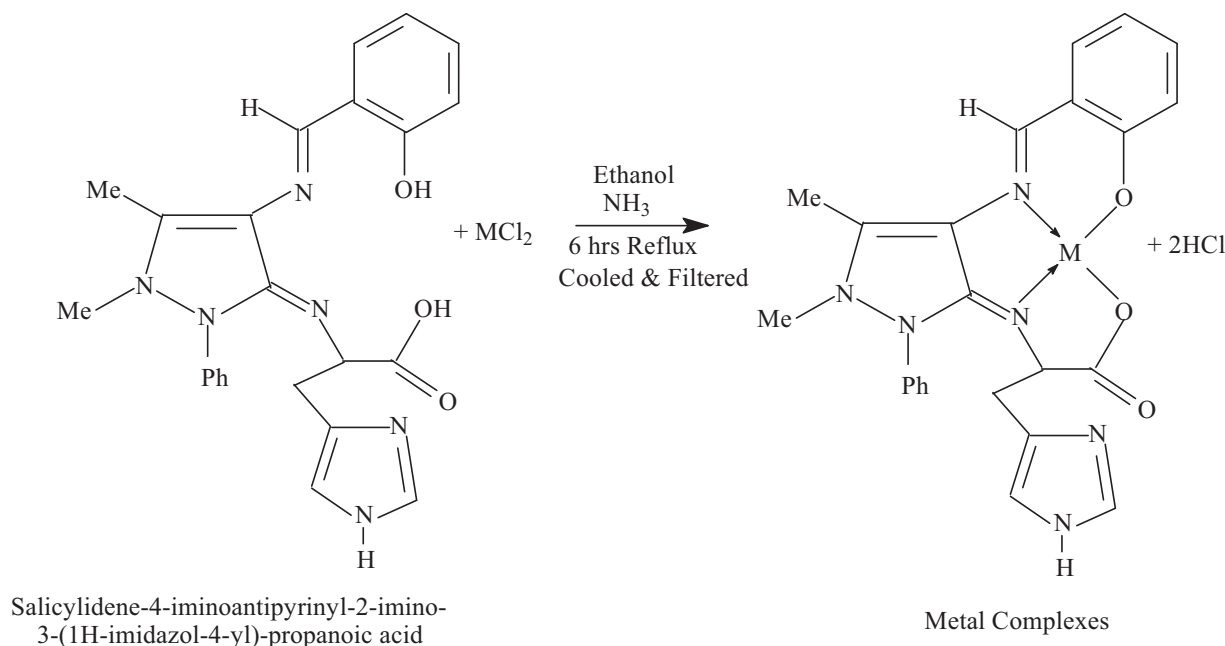
Salicylidene-4-iminoantipyrinyl-2-imino-
3-(1H-imidazol-4-yl)-propanoic acid

Metal Complexes

Where, M = Cu(II), Ni(II), Co(II), VO(IV) and Zn(II)

Scheme 2. Synthesis of Salicylidene-4-iminoantipyrinyl-2-imino-(1H-imidazol-4-yl)-propanoic acid Schiff base metal complexes.

Fig. 1. Powder XRD of (a) Schiff base, (b) [CuL], (c) [NiL] and (d) [ZnL] complexes.

3.5. ^{1}H-NMR spectral study

^{1}H-NMR spectra of Schiff base and its [ZnL] complex were recorded in CDCl$_3$ at 300 K. The Schiff base shows the peaks at 11.65 for –COOH group of histidine moiety and 9.77 ppm phenolic – OH respectively. But, the absence of these two peaks in [ZnL] complex revealed that the possible coordination of ligand system with zinc ion through –COOH and phenolic – OH group. Moreover the slight down field shift was observed for all other signals in [ZnL] complex.

3.6. UV-Vis., spectra

The UV-Vis., spectra of Schiff base shows two absorption peaks at 291 and 335 nm which are INCT transitions. The electronic absorption spectrum of [CuL] complex in acetonitrile shows a well defined band at 512 nm and a strong broad band at 803 nm which are assignable to the transitions of $^2B_{2}g \rightarrow {}^2B_1g$ and $^2B_2g \rightarrow {}^2A_1g$ respectively. Further, it shows that two main INCT bands at 298 and 342 nm regions which evident that [CuL] complex attained the square planar geometry [43].

The UV-Vis., spectra of [NiL] complex shows three bands at 293, 338 and 643 nm. With Schiff base, first two prominent bands are assignable to INCT transitions and the other one at 632 nm region which is due to $^1A_{1g} \rightarrow {}^1B_{1g}$ transition and observed magnetic moment is zero (diamagnetic) confirms square planar geometry of [NiL] complex. The three main bands were observed at 299, 326 and 617 nm regions for electronic absorption spectrum of [CoL] complex and other two strong bands in their lower wavelength regions which are assignable to INCT transitions. The d-d band at 617 nm ($^1A_{1g} \rightarrow {}^1T_{1g}$) region revealed that the presence of square planar geometry of [CoL] complex [44, 45].

The UV-Vis., spectra of [VO(IV)L] complex also recorded in MeCN solution exhibits three d-d transitions at 442 nm ($^2B_2g \rightarrow {}^2A_1g$), 614 nm ($^2B_2g \rightarrow {}^2B_1g$) and 887 nm ($^2B_2g \rightarrow {}^2Eg$) and two INCT bands (297 & 335 nm) which are supporting the square pyramidal geometry of the oxovanadium complex.

3.7. Electron Spin Resonance (ESR) spectra

X-band ESR spectra of [CuL] complex was recorded in DMSO solution at RT and LNT which shown in Fig. 3a & b [CuL] complex does not show any peaks at 1600 G which rules out of any bimolecular interaction. The anisotropic ESR parameters of [CuL] complex [g$_{ll}$ (2.33) > g$_\perp$ (2.08) > 2 and A$_{ll}$ (138) > A$_\perp$ (61)] coincide well with square planar geometey [46]. In addition, this conclusion is also supported by fact that the unpaired
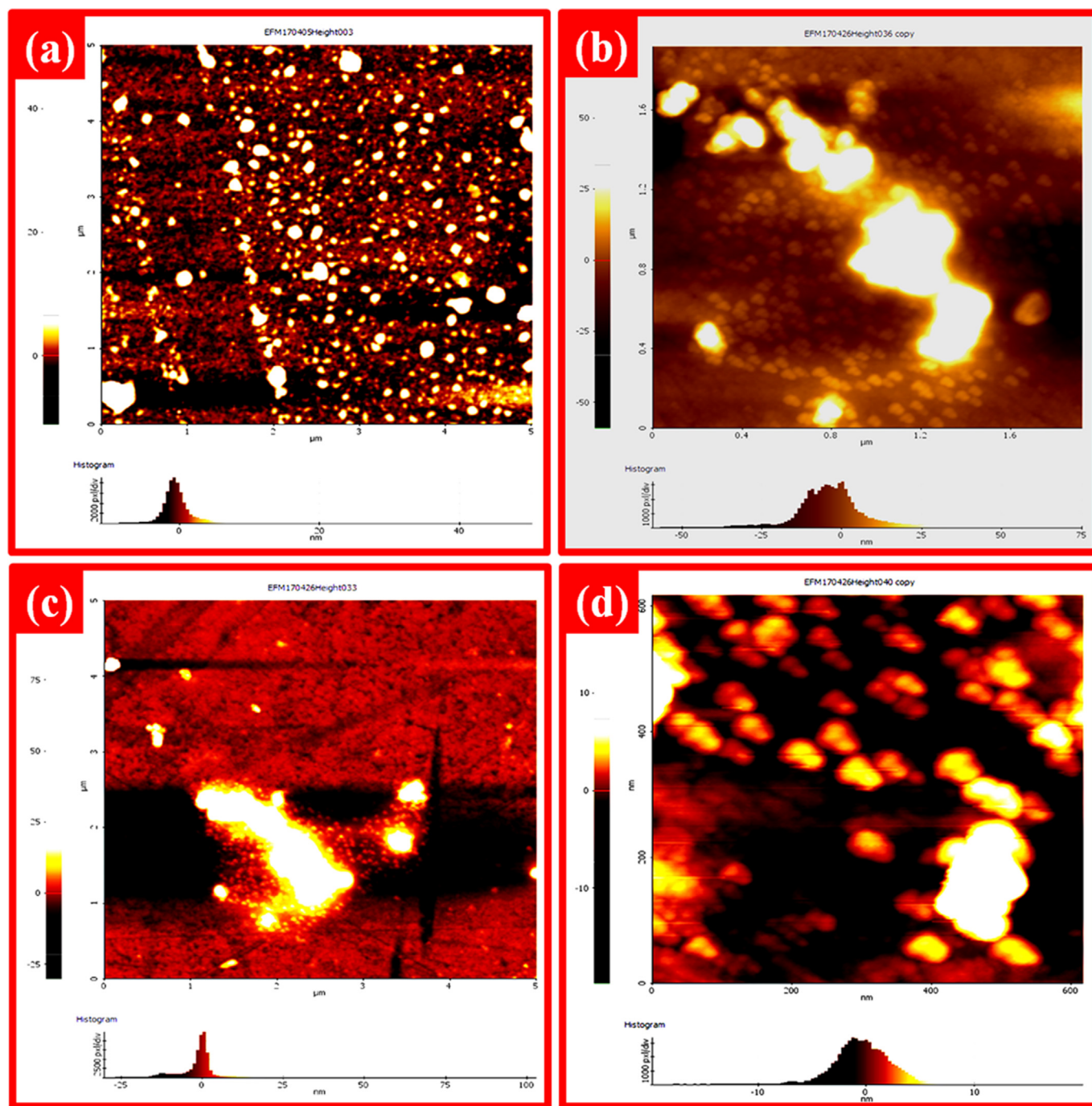
Fig. 2. AFM images of (a) Schiff base, (b) [CuL], (c) [NiL] and (d) [ZnL] complexes.

electron lies predominantly in the d_{x-y}^{22} orbital and it was evident by exchange interaction parameter (4.12). The calculated in-plane σ-bonding parameters ($\alpha^2 = 0.77$), in-plane π-bonding ($\beta^2 = 0.71$) and out-of-plane π-bonding ($\gamma^2 = 0.69$) indicates that out-of-plane π-bonding is more significant than in-plane σ-bonding and in-plane π-bonding. This is also confirmed by the orbital reduction factors [$K_{\parallel}$ (0.55) > $K_{\perp}$ (0.53)] values.

ESR spectra of [VOL] complex are recorded in DMSO solution at RT and LNT (Fig. 3c & d). The calculated spin Hamiltonian parameters from the spectra of complex ($A_{\parallel} = 182 > A_{\perp} = 74$ and $g_{\parallel} = 1.92 < g_{\perp} = 1.98$) indicates that the [VOL] complex is square pyramidal geometry. The calculated in-plane π-bonding coefficient value ($\beta^2 = 0.95$) and out-of-plane π-bonding ($\gamma^2 = 1.04$) does not deviate much from unity. This is well consistent with Kivelson's conclusion which suggests that the d_{xy}

orbital is essentially non-bonding while β^2 remain constant. The observed ($\alpha^2 = 0.86$) value indicates that the in-plane σ-bonding is significant [47, 48, 49].

3.8. Fluorescence spectra

Fluorescence spectra for Schiff base (H_2L), [CuL] and [ZnL] complexes recorded in 295 nm at 27 °C (Fig. 4). The fluorescence emission peak for Schiff base (Fig. 4a) is somewhat broaden peak at 559 nm due to INCT transitions. The sharp fluorescence emission peak of [CuL] (Fig. 4b) and [ZnL] (Fig. 4c) were observed at 553 and 556 nm. It was concluded that the emission peaks were slightly shifted to lower wavelength (red shift) region for coordination of transition metal ions with ligand. These
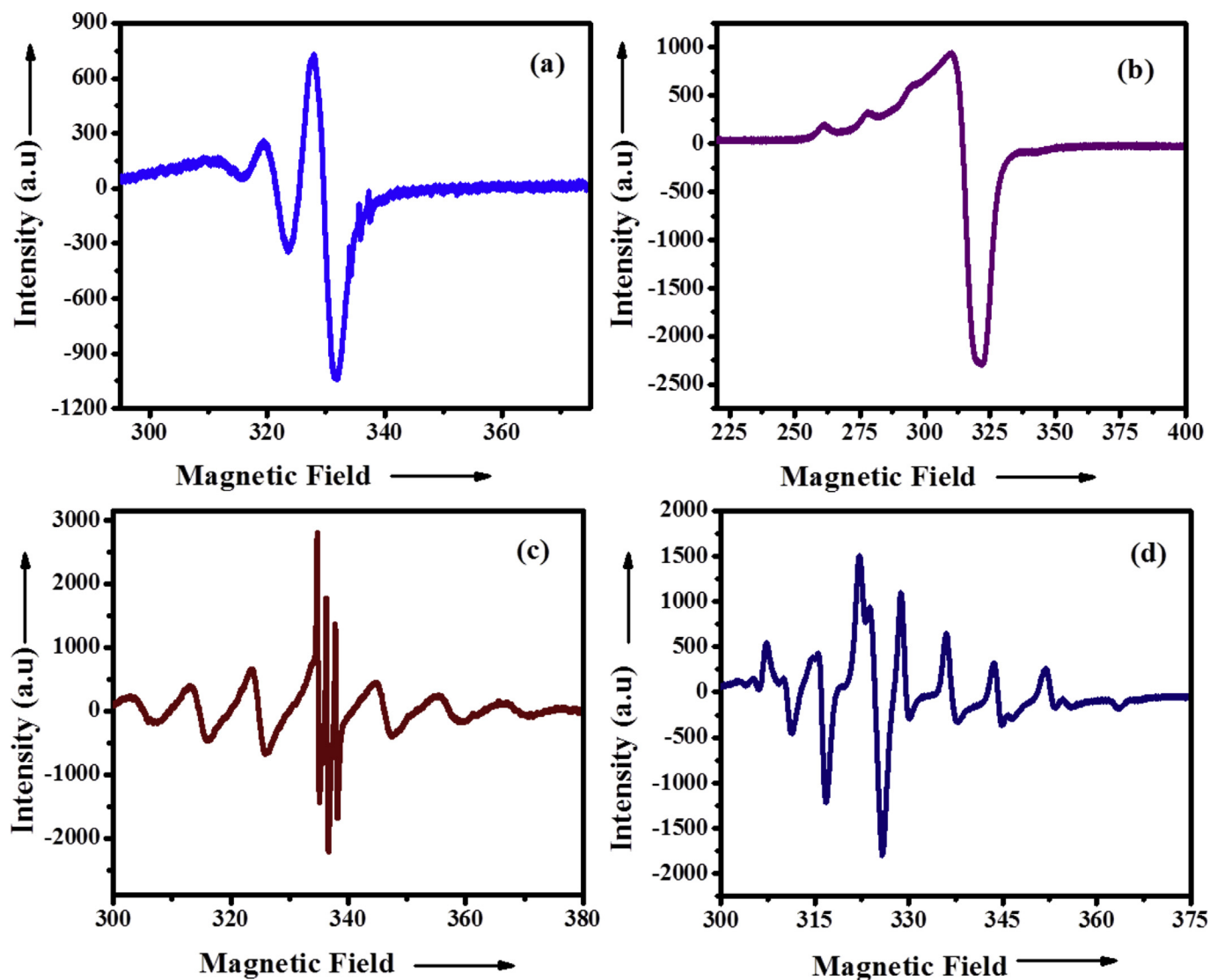
Fig. 3. X-band ESR spectra of (a & b) [CuL] and (c & d) [VOL] at RT and LNT in DMSO solution.

INCT bands of metal chelates are due to energy transfer between the HOMO (π, bonding) and LUMO (π*, antibonding) of the Schiff base in metal environment [50]. Sharp peaks with lower intensity for metal chelate reveal that the complexes have reduction in particle size upto nano scale.

3.9. UV-Visible and CV analysis for DNA interactions

The Calf Thymus-DNA interactions of synthesized compounds were evaluated by spectrophotometric titration in the presence of Tris-HCl buffer (pH = 7.3) (Fig. 5). Complex interacts with CT-DNA *via* intercalation mode which results the change in absorption intensity and peak position due to INCT bands at 261, 311 and 382 nm. In Schiff base, appearance of an isosbestic point at 295 nm is due to –OH group and it ensures the existence of its tautomeric forms with same value of molar absorptivity coefficient. The concentration of Calf Thymus-DNA increases while keeping concentration of synthesized compound which shows that exhibits their hypochromism [51]. It suggests that the interaction between Calf Thymus-DNA and synthesized compounds occurs due to the presence of hydrophobic groups in the Schiff base derivatives which also induce the hydrophobic interaction between Calf Thymus-DNA and complexes. The observed binding affinity (K_b) of Schiff

base (1.31×10^2) has been lower than the synthesized complex (1.71×10^3).

CV spectra of [CuL] complex were recorded at 300 K in presence and absences of CT-DNA at Tris-HCl buffer (pH 7.3) which shown in (Fig. 6a). In cathodic region, it shows a direct reduction peak at $Ep_c = 0.60$ V for Cu(II) → Cu(I) region. Oxidation peak was observed at $Ep_a = 0.37$ V for Cu(I) → Cu(II) region in anodic side. The strong stripping peak at $Ep_a = -0.79$ V is due to the oxidation of – C=N group in the Schiff base. This pattern was totally altered by the Calf Thymus-DNA interaction with metal ion. Decrease in intensity and increase in electrode potential of oxidation peak at $Ep_a = -0.79$ V region, reveals that CT-DNA also interact with azomethine nitrogen atom of Schiff base. CV spectra of [VO(IV)L] complex were recorded at 300 K in presence and absence of CT-DNA in Tris-HCl buffer (pH 7.3) is shown in (Fig. 6b). It shows two reduction peaks at $Ep_c = -1.18$ V for VO(II) → VO(I) and $Ep_c = 0.047$ V for VO(I) → VO(0) in cathodic region. At anodic side, direct oxidation peak was observed at $Ep_a = -0.68$ V for VO(0) → VO(II)] region which reveals that the CV spectral pattern was totally altered by CT-DNA due to strong binding with [VOL] complex. The strong stripping peak at $Ep_a = -1.31$ V is due to the oxidation of – C=N group in the Schiff base for this complex. The decrease in intensity and increase in peak potential of oxidation peak at $Ep_a = -1.31$ V region reveals that CT-DNA also interact with
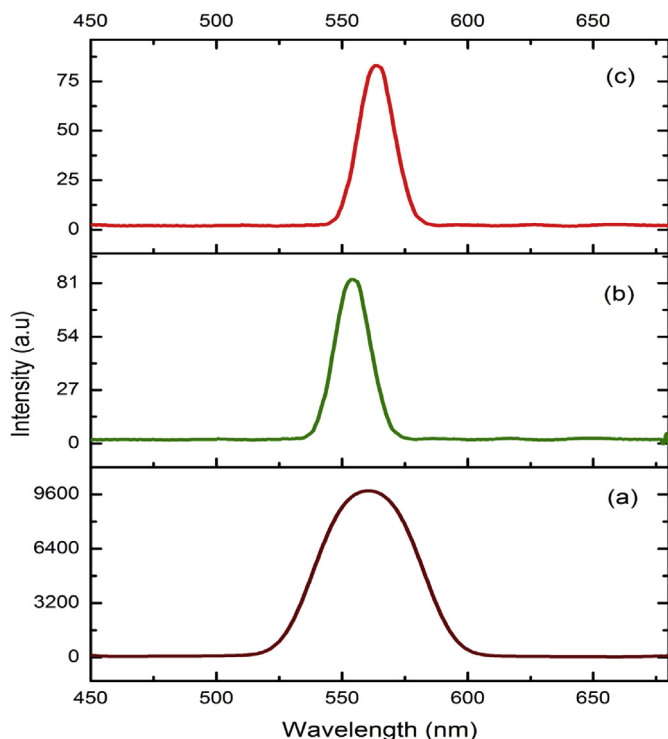
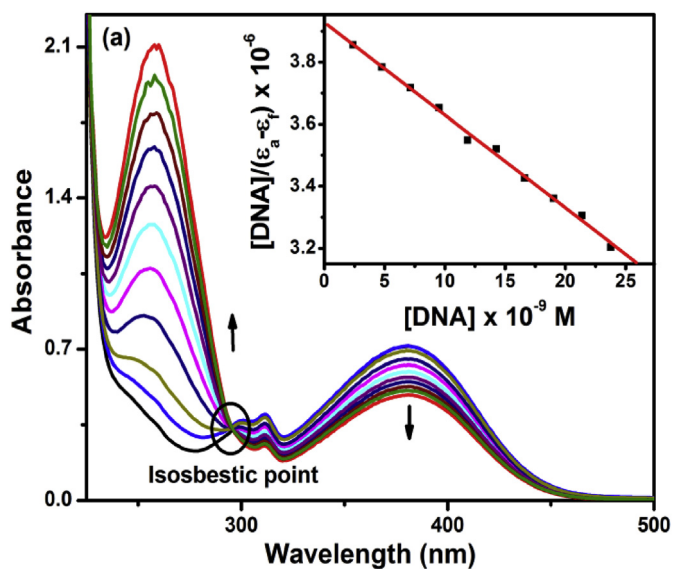**Fig. 4.** Emission spectra of (a) Schiff base, (b) [CuL] and (c) [ZnL] complexes.

Fig. 5. UV-Visible spectral study of [CuL] (1×10^{-5} M) by (0–2.5×10^{-3} M) increasing amounts of CT- DNA at RT in Tris-HCl/NaCl buffer (50 mM) (pH = 7.3). Inset $[DNA]/(\varepsilon_a-\varepsilon_f)$ x 10^{-6} Vs [DNA] x 10^{-9} plot gives to linear fit for titrating against with DNA and [CuL] complex.

azomethine nitrogen atom of Schiff base. The same observed trend in both [CuL] and [VO(IV)L] complexes concluded that the interaction of CT-DNA takes place with metal ion as well as ligand system through hydrogen bond formation.

3.10. Antimicrobial assays

Metal complexes with biological active Schiff base are a major research contract for the scientific efforts in the search of new metal based drugs, but some work is available on the bactericidal properties of
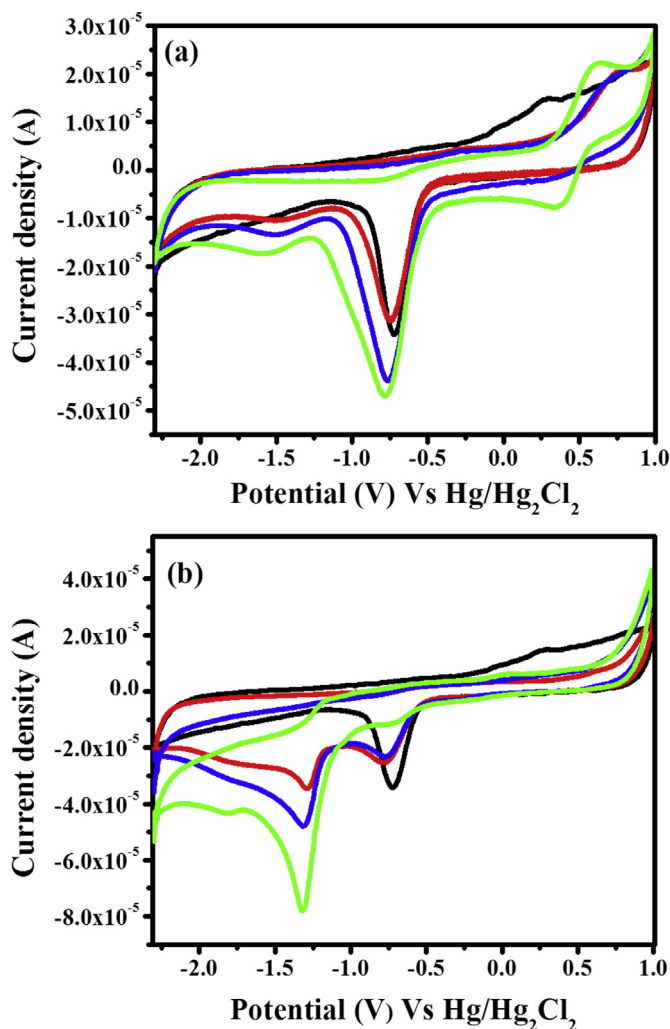

Fig. 6. CV spectra of (a) [CuL] and (b) [VOL] complexes with CT-DNA at RT by Hg/Hg_2Cl_2 used as reference electrode, Scan rate 100 mV/s in 50 mM (Tris-HCl/NaCl) Buffer (pH = 7.3).

metallic derivatives of amino acids in the literature [52]. Especially, metallic derivatives of amino acids containing N-heterocyclic bonded to the α-carbon should be studied in more detail because of the well-known role of the histidine residue binding properties. Also, it is important to study the histidine binding properties to synthesized compounds in order to provide proper evidence for essential mechanisms of biological activities. To facilitate extensive study about biological properties of synthesized compounds are discussed. An *in-vitro* antimicrobial activity results of the Schiff base metal complexes was tested against two Gram-positive (*Staphylococcus aureus* and *Bacillus subtilis*) and three Gram-negative (*Escherichia coli*, *Salmonella typhi* and *Klebsiella pneumoniae*) bacterial strains and for an *in-vitro* antifungal activity against *Aspergillus flavus*, *Candida albicans*, *Rhizoctonia bataicola*, *Rhizopus stolonifer* and *Aspergillus niger* by disc diffusion method.

The minimum inhibitory concentration (MIC) value for Schiff base metal complexes are given in Tables 2 and 3. Schiff base and its complexes show that the metals exhibited higher antimicrobial activity than the Schiff base on comparison. From MIC values, it was found that [CuL] and [VO(IV)L] were somewhat more potent among other synthesized Schiff base metal complexes.

By Overtone's concept and Tweedy's chelation theory [53, 54], such results of increased activity for the metal complexes have explained by the various researchers using different microorganisms. The lipid

Table 2
Antibacterial activity (MIC values) data of Schiff base and its metal complexes.

S.No.	Compound	Minimum Inhibitory Concentration (mg/L)				
		Staphylococcus aureus	*Escherichia coli*	*Klebsiella pneumoniae*	*Bacillus subtilis*	*Salmonella typhi*
1	H$_2$L	45	44	52	46	63
2	[CoL]	23	24	26	21	26
3	[NiL]	19	23	25	22	25
4	[CuL]	19	18	22	19	24
5	[ZnL]	15	25	24	23	29
6	[VOL]	17	16	18	15	21
7	Tetracycline*	9	8	10	7	8

* Standard.

Table 3
Antifungal activity (MIC Values) data of the Schiff base and its metal complexes.

S.No.	Compound	Minimum Inhibitory Concentration (mg/L)				
		C.albicans	*R.bataicola*	*A.flavus*	*A.niger*	*R.stolonifer*
1	H$_2$L	52	55	46	50	47
2	[CoL]	15	12	14	17	20
3	[NiL]	16	21	15	16	19
4	[CuL]	14	19	11	14	18
5	[ZnL]	17	16	13	15	16
6	[VOL]	12	17	12	13	17
7	Nystatin*	8	7	9	8	7

* Standard.

membrane that surrounds the cell positive discrimination route only the lipid-soluble resources due to which liposolubility nature is a significant factor which controls the antifungal activity results by cell permeability of overtone's theory. The metal ion polarity has reduced to a larger coverage due to overlap of the orbital (Schiff base) and partial sharing of positive charge of the metal ion with donor groups on chelating effects. Also, it increases π-electron delocalization over the intact chelate rings and as good lipophilicity of the metal complexes (Table 3). This well advanced penetration of all the metal complexes into lipid membranes and blocking of metal binding sites in the enzymes of microorganisms attained by such kinds of increasing lipophilicity [55, 56].

4. Conclusion

The neutral new tetradentate Schiff base metal complexes have prepared from the condensation of salicylidene-4-aminoantipyrine and histidine. The structural characteristic of the metal chelates have been confirmed by Analytical data, FAB-MS, ^{1}H-NMR, IR, UV, ESR, CV, Fluorescence spectra, Powder XRD data and AFM techniques. From analytical data, metal complexes correspond well with the general formula [ML]. Low molar conductance value of the metal chelates supports their neutral nature. UV-Vis., spectra evidences showed that the metal complexes are square planar geometry except [VOL] which shows square pyramidal geometry. Powder XRD data and AFM images endure that the metal complexes are nano-size grains with polycrystalline structure and the metal ions are occupying the centre position of the Schiff base. The FAB-MS of the Schiff base and metal complexes confirm the proposed stoichiometry of metal complexes. ^{1}H-NMR spectra of the Schiff base and its [ZnL] complex in CDCl$_3$ show the loss of –OH proton when complexation. ESR spectra of [CuL] and [VO(IV)L] complexes were well coinciding with reported geometries and other prepared metal complexes. CV spectra of [CuL] complex was recorded at RT which exhibits a direction reduction peak at Ep$_c$ = 0.60 V for Cu(II) → Cu(I) in the cathodic region. At anodic side, oxidation peak was observed at Ep$_a$ = 0.37 V for Cu(I) → Cu(II) region. The strong stripping peak at Epa = - 0.79 V is due to oxidation of – C=N group in the Schiff base. CV spectra of [VOL] complex were recorded at RT shows two reduction peaks at Ep$_c$ = -1.18 V for VO(II) → VO(I) and Ep$_c$ = 0.047 V for VO(I) → VO(0) in the cathodic region. At anodic side, direct oxidation peak was observed at Ep$_a$ = - 0.68 V for

VO(0) → VO(II) region. A strong stripping peak at Epa = - 1.31 V is due to oxidation of – C=N group in the Schiff base for this complex. CT-DNA interaction of [CuL] complex revealed that the binding occurs through intercalation mode between [CuL] and CT-DNA. The minimum inhibitory concentration values (MIC) against the growth of microorganisms are much higher for Schiff base than metal complexes.

Declarations

References

[1] C. Daniel, C. Fernando, P. Miguel, L.R. Gomes, J.N. Low, B. Fernanda, Development of piperic acid-based monoamine oxidase inhibitors: synthesis, structural characterization and biological evaluation, J. Mol. Struct. 1182 (2019) 298–307.

[2] A. Kulandaisamy, A. Palanimurugan, Studies on Schiff base transition metal complexes derived from benzil, p-nitroaniline and 2, 2`-bipyridyl, J. Chem. Pharm. Res. 7 (2015) 111–119.

[3] S. Esmaielzadeh, G. Mashhadiagha, Formation constants and thermodynamic parameters of bivalent Co, Ni, Cu and Zn complexes with Schiff base ligand: experimental and DFT calcualtions, Bull. Chem. Soc. Ethiop. 31 (2017) 159–170.

[4] H.L. Siddiqui, A. Iqbal, S. Ahmad, G.W. Weaver, Synthesis and spectroscopic studies of new Schiff bases, Molecules 11 (2006) 206–211.

[5] K. Shankar, J.B. Baruah, A stable peroxo- and hydroxido-bridged dinuclear cobalt(III) ethylenediamine 2,4-dinitrophenolate complex, Inorg. Chem. Commun. 84 (2017) 45–48.

[6] A. Palanimurugan, A. Kulandaisamy, DNA, in vitro antimicrobial/anticancer activities and biocidal based statistical analysis of Schiff base metal complexes derived from salicylalidene-4-imino-2,3-dimethyl-1-phenyl-3-pyrazolin-5-one and 2-aminothiazole, J. Org. Chem. 861 (2018) 263–274.

[7] W.A. Zoubi, Biological activities of Schiff bases and their complexes: a review of recent works, Int. J. Org. Chem. 3 (2013) 73–95.

[8] G. Kumaravel, P. Ponya Utthra, N. Raman, Exploiting the biological efficacy of benzimidazole based Schiff base complexes with l-Histidine as a co-ligand: combined molecular docking, DNA interaction, antimicrobial and cytotoxic studies, Bioorg. Chem. 77 (2018) 269–279.

[9] A.D. Antonik, P. Rejmak, M.T. Klepka, A. Wolska, P. Pietrzyk, K. Stępien, G. Sanna, M. Struga, Synthesis, structural studies and biological activity of novel Cu(II) complexes with thiourea derivatives of 4-azatricyclo[5.2.1.0^{2,6}]dec-8-ene-3,5-dione, J. Inorg. Biochem. 176 (2017) 8–16.

[10] A. Thakar, K. Joshi, K. Pandya, A. Pancholi, Coordination modes of a Schiff base derived from substituted 2-aminothiazole with chromium(III), manganese(II), iron(II), cobalt(II), nickel(II) and copper(II) metal ions: synthesis, spectroscopic and antimicrobial studies, E - J. Chem. 8 (2011) 1750–1764.

[11] A. Dhanalakshmi, A. Palanimurugan, B. Natarajan, Efficacy of saccharides bio-template on structural, morphological, optical and antibacterial property of ZnO nanoparticles, Mat. Sci. Eng. C 90 (2018) 95–103.

[12] P. Bhowmik, M.G.B. Drew, S. Chattopadhyay, Synthesis and characterization of nickel(II) and copper(II) complexes with tetradentate Schiff base ligands, Inorg. Chim. Acta 366 (2011) 62–67.

[13] S.Y. Ebrahimipour, I. Sheikhshoaie, A. Crochet, M. Khaleghi, K.M. Fromm, A new mixed-ligand copper(II) complex of (E)-N′-(2-hydroxybenzylidene) acetohydrazide: synthesis, characterization, NLO behavior, DFT calculation and biological activities, J. Mol. Struct. 1072 (2014) 267–276.

[14] M. Ahmed, R. Yadav, A. Sakthivel, In situ preparation, characterization, and catalytic application of various amine functionalized microporous SAPO-37, J. Nanosci. Nanotech. 16 (2016) 1–9.

[15] R. Yadav, A. Muralidhar, A. Shamna, P. Aghila, L. Gurrala, A. Sakthivel, Aluminium oxide supported on SBA-15 molecular sieves as potential Lewis acid catalysts for epoxide ring opening using aniline, Catal. Lett. 148 (2018) 1407–1415.

[16] S. Ghumaan, A. Sakthivel, D.D. Masram, M. Sathiyendiran, Electronic & magnetic properties of transition & inner transition elements & their complexes, Nova Sci. 13 (2017) 10–25.

[17] C. Karunakaran, R. Dhanalakshmi, Selectivity in photo catalysis by particulate semiconductors, Cent. Eur. J. Chem. 7 (2009) 134–138.

[18] P. Jeslin Kanaga Inba, B. Annaraj, S. Thalamuthu, M.A. Neelakantan, Salen, reduced salen and N-alkylated salen type compounds: spectral characterization, theoretical investigation and biological studies, Spectrochim. Acta Part A 104 (2013) 300–309.

[19] S. Rayati, S. Zakavi, M. Koliaei, A. Wojtczak, A. Kozakiewicz, Electron-rich salen-type Schiff base complexes of Cu(II) as catalysts for oxidation of cyclooctene and styrene with tert-butylhydroperoxide: a comparison with electron-deficient ones, Inorg. Chem. Commun. 13 (2010) 203–207.

[20] D. Emadi, M.R. Yaftian, S. Rayati, N,N'-Bis(1'-hydroxy-2'-acetonaphthone) propylenediamine: synthesis, extractive properties, and use as an ionophore in a Cu(II)-selective potentiometric sensor, Turk. J. Chem. 31 (2007) 423–433.

[21] A.E. Patterson, J.J. Miller, B.A. Miles, E.L. Stewart, J.M.E.J. Melanson, C.M. Vogels, A.M. Cockshutt, A. Decken, P.M. Jr, S.A. Westcott, Synthesis, characterization and anticancer properties of (salicylaldiminato)platinum(II) complexes, Inorg. Chim. Acta 415 (2014) 88–94.

[22] A. Ghaleb, M. El Amane, Y. Kennouche, H. El Hamdani, M. Bouhdada, M. Ahmami, Synthesis and characterisation of the mixed ligand complexes, [M(ox)(caf)₂], H₂O, M=Cu²⁺, Zn²⁺, Mn⁺², Fe²⁺, Cd²⁺, Co²⁺, Ni²⁺; ox=oxalato; caf=caffeine, J. Appl. Chem. 5 (2016) 670–677.

[23] F. Silva, C. Fernandes, M.P.C. Campello, A. Paulo, Metal complexes of tridentate tripod ligands in medical imaging and therapy, Polyhedron 125 (2017) 186–205.

[24] A. Dhanalakshmi, B. Natarajan, V. Ramadas, A. Palanimurugan, S. Thanikaikarasan, Structural, morphological, optical and antibacterial activity of rod-shaped zinc oxide and manganese-doped zinc oxide nanoparticles, Pramana - J. Phys. 87 (2016) 1–9.

[25] Z. Tohidiyan, I. Sheikhshoaie, M. Khaleghi, Two new Cu(II) and Zn(II) Schiff base complexes: synthesis, characterization and their biological activity, Int. J. Nano Dimens. 7 (2016) 127–136.

[26] T. Baskaran, A. Joshi, G. Kamalakar, A. Sakthivel, A solvent free method for preparation of β-amino alcohols by ring opening of epoxides with amines using MCM-22 as a catalyst, Appl. Catal. A 524 (2016) 50–55.

[27] A. Dhanalakshmi, A. Palanimurugan, B. Natarajan, Enhanced antibacterial effect using carbohydrates biotemplate of ZnO nano thin films, Carbohydr. Polym. 168 (2017) 191–200.

[28] N. Revathi, M. Sankarganesh, J. Rajesh, J. Dhaveethu Raja, Biologically active Cu(II), Co(II), Ni(II) and Zn(II) complexes of pyrimidine derivative Schiff base: DNA binding, antioxidant, antibacterial and in vitro anticancer studies, J. Fluoresc. 27 (2017) 1801–1814.

[29] A. Palanimurugan, A. Kulandaisamy, Biological screening studies of DNA relate metal complexes from benzylidene-4-imino-2,3-dimethyl-1-phenyl-3-pyrazolin-5-one and 2-aminothiazole, Asian J. Chem. 30 (2018) 594–602.

[30] S. Sujarani, A. Ramu, Docking of ethanamine Schiff base imines & metal (II) complexes, cytotoxicity & DNA interaction studies, J. Mol. Struct. 1079 (2015) 353–362.

[31] S. Kongchoo, K. Chainok, A. Kantacha, S. Wongnaw, Copper(II) complex as a precursor for formation of cyano-bridged pentanuclear Fe^{III}-Cu^{II}bimetallic assembly: synthesis, characterization, crystal structure and antibacterial activity, J. Chem. Sci. 129 (2017) 431–440.

[32] A. Palanimurugan, V. Sudharkani, A. Kulandaisamy, Synthesis, spectral, redox and antimicrobial activities of mixed ligand complexes derived from 1-phenyl-2,3-dimethyl-4-imino-benzylidene-pyrazol-5-one and dimethylglyoxime, J. Nanosci. Tech. 2 (2016) 204–208.

[33] V. Kumar, N.J. Turro, J.K. Barton, Photophysics of ruthenium complexes bound to double helical DNA, J. Am. Chem. Soc. 107 (1985) 5518–5523.

[34] N. Raman, C. Thangaraja, S. Johnsonraja, Synthesis, spectral characterization, redox and antimicrobial activities of Schiff base transition metal (II) complexes derived from 4-aminoantipyrine and 3-salicylideneacetylacetone, Cent. Eur. J. Chem. 3 (2005) 537–555.

[35] F.E. Smith, R.C. Hynes, T.T. Ang, L.E. Khoo, G. Eng, The synthesis and structural characterization of a series of pentacoordinate diorganotin(IV) N-arylidene-α-amino acid complexes, Can. J. Chem. 70 (1992) 1114–1120.

[36] J. Joseph, K. Nagashri, G. Ayisha, B. Rani, Synthesis, characterization and antimicrobial activities of copper complexes derived from 4-aminoantipyrine derivatives, J. Saudi Chem. Soc. 17 (2013) 285–294.

[37] N. Raman, S.J. Raja, A. Sakthivel, Transition metal complexes with Schiff-base ligands; 4-aminoantipyrin based derivatives – a review, J. Coord. Chem. 62 (2009) 691–709.

[38] M. Gielen, M. Biesemans, R. Willem, Organotin compounds: from kinetics to stereochemistry and antitumour activities, Appl. Organomet. Chem. 19 (2005) 440–450.

[39] A. Palanimurugan, A. Kulandaisamy, Synthesis, characterization, antimicrobial and anticancer activities of 14-membered macrocyclic Schiff base metal complexes, Asian J. Chem. 30 (2018) 1262–1268.

[40] R. Willem, I. Verbruggen, M. Gielen, Correlating Mössbauer and solution- and solid-state ^{117}Sn NMR data with X-ray diffraction structural data of triorganotin 2-[(E)-2-(2-hydroxy-5-methylphenyl)-1-diazenyl]benzoates, Organ 17 (1998) 5758–5766.

[41] B.H.M. Hussein, M.A. Gouda, W. Fathalla, S. Arabi, Europium-(7-carboxymethoxy-4-methyl coumarin)2 complex based electrochemical probe for DNA based on the interaction between them, J. New Mat. Electrochem. Syst. 20 (2017) 189–195.

[42] V. Prakash, M.S. Suresh, Preparation characterization, ^{1}H, ^{13}C NMR study and antibacterial studies of Schiff bases and their Zn(II) chelates, Res. J. Pharmaceut. Biol. Chem. Sci. 4 (2013) 1536–1550.

[43] S. Ramakrishnan, M. Palaniandavar, Mixed ligand copper (II) complexes of dipicolylamine and 1, 10-phenanthroline: the role of diimines in the interaction of the complexes with DNA, J. Chem. Sci. 117 (2015) 179–186.

[44] K. Singh, R. Thakur, G. Kumar, Synthesis, characterization and in vitro anticancer activity of Co(II), Ni(II), Cu(II) and Zn(II) complexes with bidentate Schiff base 4-[{3-(4-bromopheyl)-1-pheyl 1H-pyrazol-4ylmethylene}-amino]-3-mercapto-1,2,4-triazin-5-one, Eur. Chem. Bull. 5 (2016) 46–53.

[45] A. Karaliota, O. Kretsi, C. Tzougraki, Synthesis and characterization of a binuclear coumarin-3-carboxylate copper(II) complex, J. Inorg. Biochem. 84 (2001) 33–37.

[46] I. Kostova, I. Manolov, I. Nicolova, S. Konstantinov, M. Karaivanova, New lanthanide complexes of 4-methyl-7-hydroxycoumarin and their pharmacological activity, Eur. J. Med. Chem. 36 (2001) 339–347.

[47] H.A. Azab, Z.M. Anwar, R.G. Ahmed, Pyrimidine and purine mononucleotides recognition by trivalent lanthanide complexes with N-acetyl amino acids, J. Chem. Eng. Data 55 (2010) 459–475.

[48] H.A. Azab, B.H.M. Hussein, A.I. El-Falouji, Synthesis of novel Eu(III) luminescent probe based on 9-acridine carboxylic acid skeleton for sensing of ds-DNA, J. Fluoresc. 22 (2012) 639–649.

[49] C. Stefano, B. Marco, C. Barbara, A new convenient route to 2-oxoethoxycoumarins: key intermediates in the synthesis of natural products, Tetrahedron 58 (2002) 4851–4858.

[50] S. Shanthi, S.S. Mansoor, Kinetics and mechanism of oxidation of some α-hydroxy acids by tripropylammonium fluorochromate in aqueous acetic acid medium, Chem. Sci. Trans. 4 (2015) 213–221.

[51] K.J. Humphreys, K.D. Karlin, S.E. Rokita, Efficient and specific strand scission of DNA by a dinuclear copper complex: comparative reactivity of complexes with linked tris(2-pyridylmethyl)amine moieties, J. Am. Chem. Soc. 124 (2002) 6009–6019.

[52] S.B. Nimse, D. Pal, Free radicals, natural antioxidants, and their reaction mechanisms, RSC Adv. 5 (2015) 27986–28006.

[53] D.J. De Geest, A. Noble, B. Moubaraki, K.S. Murray, D.S. Larsen, S. Brooker, Dicopper(II) complexes of a new pyrazolate-containing Schiff-base macrocycle and related acyclic ligand, Dalton Trans. 28 (2007) 467–475.

[54] R.N. Patel, Synthesis, characterization and superoxide dismutase activity of some four coordinated copper(II) complexes, Indian J. Chem. Sect. A 48 (2009) 1370–1377.

[55] N. Demirezen, D. Tarinc, D. Polat, M. Cesme, A. Golcu, M. Tumer, Synthesis of trimethoprim metal complexes: spectral, electrochemical, thermal, DNA-binding and surface morphology studies, Spectrochim. Acta 94 (2012) 243–255.

[56] E.A. Al-Razaq, O.M. Al-Ramadany, M.A. Al-Shama, T.A.K. Al-Allaf, Synthesis and characterization of organ silicon (IV) complexes with some Schiff base derivatives, Int. J. Chem. Sci. 3 (2005) 253–262.